ISSN 0003-6838, Applied Biochemistry and Microbiology, 2010, Vol. 46, No. 7, pp. 671–687. © Pleiades Publishing, Inc., 2010.
Original Russian Text © V.A. Likhoshvai, T.M. Khlebodarova, M.T. Ree, N.A. Kolchanov, 2009, published in Biotekhnologiya, 2009, No. 4, pp. 8–29.

Metabolic Engineering in Silico

V. A. Likhoshvai[a, b], T. M. Khlebodarova[a], M. T. Ree[a], and N. A. Kolchanov[a, b]

[a] *Institute of Cytology and Genetics, Siberian Branch, Russian Academy of Sciences, Novosibirsk, 630090 Russia*
e-mail: tamara@bionet.nsc.ru, likho@bionet.nsc.ru
[b] *Novosibirsk State University, Novosibirsk, 630090 Russia*

Received June 24, 2009

Abstract—This review briefs on the main directions in the field of mathematical modeling of metabolic processes aimed at a rational design of genetically modified organisms. The class of generalized Hill functions is described, and their application to modeling of nonlinear processes in *Escherichia coli* metabolic systems is illustrated by several examples. A model for the pyrimidine biosynthesis in *E. coli*, taking into account the nonlinear effects of a negative allosteric regulation of enzyme activities involved in the control of the subsequent stages by the end products of synthesis, is considered. It has been shown that the model displays its own continuous oscillation mode of functioning with a period of approximately 50 min, which is close to the duration of *E. coli* cell cycle. The need in considering the nonlinear effects in the models as essential elements in the function of metabolic systems far from equilibrium is discussed.

Key words: mathematical modeling, metabolic engineering, generalized Hill functions, regulation, *Escherichia coli*.

DOI: 10.1134/S0003683810070021

Metabolic engineering is a methodology in state-of-the-art biotechnology which is widely used for designing producers of biologically active substances involving industrially important microorganisms [1–14]. Practical importance of this direction could be hardly overestimated, since it is directly connected with the quality of contemporary human life. Design of producers is impossible without development of the methods for targeted impact on individual stages of the process to increase the yield of the final product. Currently there are experimental approaches for solving such problems [15]; however, the selection of particular impact in each particular case without an integrated estimation of its results is complex and ambiguous [16, 17]. From the basic standpoint, this is one of the most complex problems in optimization of cell function in a necessary direction in a changed genetic environment.

Mathematical modeling occupies a key position in metabolic engineering [18, 19] starting from the works of J. Bailey and M. Shuler et al. on modeling of the overall *E. coli* cell metabolism in the 1980s [20–23]. Construction of adequate mathematical models for the metabolism of target biological objects provides for a systems analysis of metabolic networks and prediction of their behavior after an impact, which considerably enhances the design of producer strains and optimization of their functioning [24–32]. These possibilities are determined by the advantages characteristic of mathematical models. First, they provide for synthesis of the experimental data for various levels in organization of biological systems and under various conditions. Second, an integrated conceptual model unites in a natural manner all the levels in organization of biological systems thereby creating the possibilities to analyze the cause–effect relationships between molecular structure, dynamics, and phenotypic characteristics of the system. Third, mathematical models make it possible to develop computer systems for in silico experiments, i.e., for studying target model biological systems in space and time.

Various modeling strategies and various approaches are currently used when analyzing cells of both prokaryotic and eukaryotic organisms, which, possessing certain advantages and limitations, provide for solution of a stated problem in each particular case. Among the most widespread approaches in this field is

Abbreviations: MTO—model of target objects, GHF—generalized Hill function, AKB—α-ketobutyrate, APRT—adenine phosphoribosyltransferase, ATCase—aspartate transcarbamoylase, CAASP—carbamoyl aspartate, CAP—carbamoyl phosphate, CPSase—carbamoyl phosphate synthetase, CTPase—cytosine triphosphate synthetase, DAHPS(Trp)—tryptophan-sensitive 3-deoxy-D-arabinoheptulonate-7-phosphate synthetase, 3DDAH7P—3-deoxy-D-arabinoheptulonate-7-phosphate, DHOase—dihydroorotate dehydrogenase, DOROA—dihydroorotate, E4P—erythrose-4-phosphate, Lac—lactate, LDHA—NAD(P)-dependent lactate dehydrogenase 2, NDK—nucleoside diphosphate kinase, OMP—orotidine monophosphate, OMPase—orotidine monophosphate decarboxylase, OPTase—orotate phosphoribosyl transferase, OROA—orotate, Ox—oxalate, PEP—phosphoenolpyruvate, PFL1—pyruvate formate lyase, Pyr—pyruvate, RDREDase—ribonucleoside diphosphate reductase, RNTPRase—ribonucleoside triphosphate reductase, Trp—tryptophan, UMP kinase—uridine monophosphate kinase.

stoichiometric modeling of cell metabolism (flux balance models), which describes functioning of metabolic networks in assumption that the processes occurring in these networks are either in a quasi-stationary state or close to this state [33–40]. The advantage of such models inherently follows from this approach, which describes a process or a function of an entire cell only via the fluxes of metabolites without taking into account the details of the corresponding mechanisms, thereby allowing the largest hindrance encountered by developers of dynamic models for biological systems to be overcome, namely, an insufficient description of the dynamics of kinetic processed in the cell. This research direction is represented by rather numerous papers on metabolic engineering; flux models are successfully enough used for design and optimization of various processes of biosynthesis, including the biosyntheses of lysine [41–43] and L-methionine [28] in *Corynebacterium glutamicum* cells; of butyric acid [44–46] in *Clostridium acetobutylicum* cells; and ethanol [24], succinic acid [47, 48], 1,3-propanediol [47], amino acids [28, 49], lactic acid [47, 50, 51], and other substances in *E. coli* cells. Stoichiometric modeling of cell processes is widely used for predicting the level of biosynthesis for technologically important products depending on the conditions for cell growth and other impacts as well as for optimization of cell growth conditions on various substrates [30, 33, 43, 52].

Flux models and their use for computing the balance of metabolic fluxes (flux balance approach) were proposed by several researchers as early as the 1980s for modeling the production of butyric acid in *Clostridium acetobutylicum* cells [44] and lysine in *Corynebacterium glutamicum* cells [41], and glucose metabolism in bacterial cells [53] and were further developed by Palsson et al. [33–35, 37, 50, 52, 54–58] and other researchers [39, 42]. The flux model is a set of linear differential equations describing the system of interacting metabolites based on a stoichiometric matrix. The flux balance equations are put down as the equality between the total rate of metabolite fluxes for all reactions where they are produced and the total rate of their outflow to all the reactions where they are utilized [33, 39]. In a certain sense, these models describe the physiology of cell metabolism; in this case, any analysis of the molecular mechanisms underlying the functioning of a system is out of question. To increase the efficiency of stoichiometric models applied to analysis, prediction, and optimization of producer expression, additional methods are used [29, 30, 47, 49, 59] and hybrid models combining various approaches are developed [60].

Despite such a wide application of flux balance modeling in metabolic engineering, *dynamic models*, based on the kinetic methods, have not lost their attraction as a tool for analysis of the mechanisms underlying behavior of a system [31, 61–63]. Among the hindrances encountered by developers of such models are insufficient data for verifying the constructed models. Sometimes it becomes an insurmountable obstacle for construction of an adequate mathematical model for a studied metabolic process or the genetic system controlling the corresponding process. Consequently, a topical problem is to develop methods and approaches that would provide for construction of adequate dynamic models with forecasting abilities allowing the behavior of a metabolic system after introduction of particular genetic changes to be predicted. Several different approaches are currently used for describing reaction kinetics that make it possible, at least in part, to overcome the above described difficulties. Among them are generalized description of reaction rates [64] using linear approximation [65] as well as the use of linear logarithmic functions [66], thermokinetic description of reaction rates [67], the use of lin-log approximations [27, 29, 68–70], S systems, and other methods [71–74].

We are developing a generalized chemical kinetic approach based on description of the behavior dynamics of a metabolic or molecular genetic system with the help of nonlinear differential equations with their right-hand members constructed using generalized Hill functions (GHFs) [75–78]. In this approach, any metabolic network is considered as an interconnected system comprising elementary subsystems, namely, enzymatic reactions; genetic elements coding for proteins and RNA; subsystems of RNA synthesis, modification, and degradation; and others. Modeling consists in development of the background, namely, models of elementary subsystems, and using these models as bricks for constructing the models of target objects (MTOs). Each elementary model describes a pattern for change in the rate of synthesis or utilization of a certain group of substances. The MTO is assembled based on the law for summing the local rates determined by the elementary models included in this MTO. Currently, we use the generalized Hill functions for creation of the database on models of enzymatic reactions in the *E. coli* cell and develop the models for expression regulation of the genes encoding enzymes and their subunits [79]. The database on models will in the future provide for construction of a large-scale model of *E. coli* metabolism, which will take into account the nonlinear mechanisms involved in the regulation of gene expression and enzyme activities. So far, we have developed approximately 370 models for enzymatic reactions (approximately 30% of all reactions), 23 metabolic pathways providing for cell respiration and energy supply (glycolysis, tricarboxylic acid cycle, and pentose phosphate cycle), metabolisms of pyruvate and hydrocarbon nutrition sources, membrane transport, biosynthesis and degradation of several amino acids (alanine, asparagine, arginine, cysteine, glutamine, methionine, proline, threonine, lysine, etc.), biosynthesis of nucleic acids, and some other metabolic pathways [77, 79–82]. We have also constructed models for functioning of approximately 20 promoters. Concurrently, we are involved in construction and analysis of mathematical models for individual metabolic pathways. Below are some exam-

ples of elementary models as well as a brief description of the mathematical model for biosynthesis of nucleotides. These examples demonstrate the potential of the developed method in describing the kinetics of nonlinear enzymatic processes and show that the nonlinear effects in regulation of enzyme activities lead to oscillations of instantaneous concentrations of metabolites.

BRIEF DESCRIPTION OF THE METHOD OF GENERALIZED HILL FUNCTIONS

Insufficient data on the mechanisms underlying the functioning of an elementary subsystem frequently interfere with construction of its detailed model. In such situations, it is reasonable to construct approximating models, which are mainly based on kinetic data, while the available data on the structure–function organization of the subsystem play a supporting role or are not considered at all [78]. The models that approximate the rates of processes in elementary subsystems can be constructed with the help of various classes of functions. In particular, the kinetic data themselves on the changes in rates depending on external parameters can be considered as a model. This type of models is specified as a table. In the case of table models, the values in the absent experimental points are computed based on approximation with polynomials, spline functions, and piecewise constant or piecewise linear functions. Therefore, it is purposeful in modeling practice to replace table models with continuous approximating models. Generally speaking, the approximation approach does not require any knowledge about the mechanisms of a considered process. A control law can be reconstructed directly from kinetic curves, while its variables and parameters correspond only to the values measured in experiment. Consequently, an approximating model of an elementary subsystem operates with a minimal number of variables. The class of GHFs is used to construct approximating models for elementary subsystems in the context of our approach; these functions are an extension of the class of rational polynomials derived when modeling enzymatic reactions [83]. The need in expanding the class of rational polynomials is dictated by the presence of the systems that function with variable Hill coefficients [84].

Define the generalized Hill functions in an iteration manner as

(1) A rational polynomial

$$h(X) = \sum_{\alpha \in A} \delta_\alpha \prod_{\alpha \in X_\alpha} (x/k_{1,\alpha})^{h_{\alpha,X}} / \sum_{\alpha \in A} \prod_{\alpha \in X_\alpha} (x/k_{2,\alpha})^{h_{\alpha,X}}$$

with nonnegative parameters δ_α, $k_{1,\alpha}$, $k_{2,\alpha}$, and $h_{\alpha,X}$ is a GHF.

(2) The function obtained from the function from paragraph (1) by substituting a GHF for its variables and parameters is a GHF.

(3) A product and a sum of generalized functions are generalized functions.

X stands for the set of nonnegative variables x. The parameters $k_{1,\alpha}$ and $k_{2,\alpha}$ are dimensional. Their dimensionality coincides with the dimensionality of variables x. These constants specify the generalized efficiencies of the influence of a group of factors $x \in X_\alpha$ on the described process. The parameters δ_α and $h_{\alpha,X}$ are dimensionless: the parameters $h_{\alpha,X}$ specify the degree of nonlinearity (cooperativeness) of the effect of substance x on the process and are regarded as Hill coefficients; the parameters δ_α acquire the value of zero or unity and specify the type of the effect of a substance or group of substances on the process rate (if $\delta_\alpha = 0$, then the effect is strictly negative, and if $\delta_\alpha = 1$, the effect can be either negative or positive depending on the values of parameters $k_{1,\alpha}$ and $k_{2,\alpha}$.

The use of GHFs for description of the rates of processes in elementary subsystems constituting target objects (including the rates of enzymatic reactions in metabolic pathways) in the case of insufficient data on their structure–function organization provides for reconciling the number of variables and parameters of the model with the available data, which is important when searching for optimal values of model parameters [77, 78]. There are yet no algorithms for construction of an optimal GHF based on kinetic data; therefore, construction of each equation is an unformalizable process requiring participation of an expert. Below we demonstrate derivation of equation by the example of description of the oxygen action on the activity of promoter in cyoABCDE operon. The remaining equations are demonstrated without detailing the procedures used to derive them.

ELEMENTARY MODELS OF *E. coli* METABOLIC SUBSYSTEMS

A model of the reaction catalyzed by tryptophan-sensitive 3-deoxy-D-arabinoheptulonate-7-phosphate synthetase. DAHPS(Trp) is one of the three isozymes that catalyze the first step in the metabolic pathways providing for the biosynthesis of aromatic amines in an *E. coli* cell, namely, condensation of phosphoenolpyruvate (PEP) and erythrose-4-phosphate (E4P) into 3-deoxy-D-arabinoheptulonate-7-phosphate (3DDAH7P). This reaction can be presented in a general form as E4P + PEP + H_2) ⟶ 3DDAH7P.

GHFs with variable coefficients were used to construct the model for the enzymatic reaction catalyzed by DAHPS(Trp), encoded by the *E. coli* gene *aroH*. The model was verified using the kinetic data from [84].

Tryptophan-sensitive DAHPS(Trp) is a homodimer, has two substrate-binding sites, and is activated by bivalent metals. This enzyme demonstrates a sigmoid activity kinetics, which depends on the concentrations of both substrates, E4P and PEP. Its catalytic activity and affinity for substrates depend on the type of metal ions. At low E4P concentrations, the binding of L-tryptophan (Trp) to enzyme elevates its activity, decreases k_{cat}, and increases the affinity for both substrates; however, a positive cooperativity of

the interaction with substrates decreases [84]. The enzymatic reaction catalyzed by this enzyme has a very intricate Trp-regulated mechanism. To describe the Trp action on the enzyme activity, we used GHF (1) with variable Hill coefficients:

$$V = \frac{k_{\text{cat}} e_0 (S_1/K_{S_1})^{h_{S_1}} (S_2/K_{m,S_2})^{h_{S_2}}}{P_2/K_{i,P_2} + [1 + (S_1/K_{S_1})^{h_{S_1}}][1 + (S_2/K_{m,S_2})^{h_{S_2}}]} f_1,$$

$$f_1 = \frac{1}{1 + kI_{R,V_{\max}} \dfrac{R}{k_{R,V_{\max}} + R}},$$

$$K_{S_1} = \frac{K_{m,S_1}}{1 + kI_{R,K_{m,S_1}} \dfrac{R^{h_{R,K_{m,S_1}}}}{k_{R,K_{m,S_1}}^{h_{R,K_{m,S_1}}} + R^{h_{R,K_{m,S_1}}}}}, \quad (1)$$

$$h_{S_1} = \frac{h_{0,S_1}}{1 + kI_{R,h_{S_1}} \dfrac{R^{h_{R,h_{S_1}}}}{k_{R,h_{S_1}}^{h_{R,h_{S_1}}} + R^{h_{R,h_{S_1}}}}},$$

$$h_{S_2} = \frac{h_{0,S_2}}{1 + kI_{R,h_{S_2}} \dfrac{R^{h_{R,h_{S_2}}}}{k_{R,h_{S_2}}^{h_{R,h_{S_2}}} + R^{h_{R,h_{S_2}}}}}.$$

In model (1), V is reaction rate; e_0 is concentration of enzyme; and S_1, S_2, P_1, P_2, and R are concentrations of E4P, PEP, inorganic phosphate PI, 3DDAH7P, and TRP, respectively. A characteristic feature of this model is that the parameters K_{S_1}, K_{S_2}, h_{S_1}, and h_{S_2} are the variables depending on current tryptophan concentration. This is how the complexity of the mechanism underlying DAHPS(Trp) function manifests itself.

Figure 1 shows the computation results for the enzyme activity according to model (1) compared to the experimental data on the effects of various Trp concentrations on the rate of the reaction catalyzed by the enzyme DAHPS(Trp) at fixed substrate concentrations, (a) PEP = 150 μM and (b) E4P = 300 μM.

A model for activity regulation of adenine phosphoribosyltransferase (APRT) by nucleoside-5'-phosphates. Adenine phosphoribosyltransferase (AMP:pyrophosphate phosphoribosyltransferase, EC 2.4.2.7) in *E. coli* cells catalyzes reutilization of free adenine (A). Use of the 5-phosphoribosyl-1-pyrophosphate (PRPP) as a second substrate in this reaction yields AMP and pyrophosphate (PPI). In a general form, this reaction can be put down as A + PRPP ⟶ PPI + AMP.

The model of this enzymatic reaction catalyzed by the *E. coli* APRT was constructed using the kinetic data from [85]. It is known that all noncyclic nucleoside-5'-phosphates to a considerable degree inhibit APRT activity via competition with the substrate PRPP [85]. The model for a stationary rate of this enzymatic reaction is described by the following equation:

$$V = \frac{k_{\text{cat}} e_0 \dfrac{S_1}{K_{m,S_1}} \dfrac{S_2}{K_{m,S_2}}}{\left(1 + \dfrac{S_1}{K_{m,S_1}}\right)\left(1 + \dfrac{S_2}{K_{m,S_2}} + \dfrac{P_1}{K_{i,P_1}} + \dfrac{P_2}{K_{i,P_2}} + \sum_{j=1}^{5} \dfrac{R_j}{K_{i,R_j,S_2}} + \sum_{j=6}^{10} \left(\dfrac{R_j}{K_{i,R_j,S_2}}\right)^2 + \dfrac{R_{11}}{k_{i,R_{11},S_2}}\right)} \frac{1}{1 + kI_{R_{12}} \dfrac{R_{12}}{k_{R_{12}} + R_{12}}}, \quad (2)$$

where e_0 is the concentration of enzyme APRT and S_1, S_2, P_1, P^2, R_1, R_2, R_3, R_4, R_5, R_6, R_7, R_8, R_9, R_{10}, R_{11}, and R_{12} are the concentrations of low-molecular-weight substances A, PRPP, PPI, AMP, ADP, dADP, ATP, dATP, dAMP, GTP, ITP, xanthine triphosphate (XTP), UTP, GDP, Mg^{2+}, and cAMP, respectively. Figure 2 demonstrates the computation results obtained using model (2) for the dynamics of APRT activity depending on concentrations of various low-molecular-weight substances (R_i) compared to the corresponding experimental data [85].

The enzymatic reaction catalyzed by APRT demonstrates how multicomponent and nontrivial can be the regulation of a molecular system in the cell on the background of structural similarity between its numerous components. Such property of subsystems can also come out of a tremendous number of nonspecific interactions in the cell. Thus, the considered enzymatic system affects a basic property of the cell. It is of paramount importance for an adequate description of real molecular processes proceeding in the cell in vivo to take into account such specific features in modeling of molecular genetic systems.

A model of activity regulation of the key enzyme in pyruvate metabolism, *E. coli* lactate dehydrogenase 2. Under anaerobic conditions, the distribution of carbon fluxes in the *E. coli* cell is the result of the competition for pyruvate between two key enzymes, KAO(P)-dependent lactate dehydrogenase (LDHA) and pyruvate formate lyase (PFL1). LDHA converts pyruvate into D-lactate, and PFL1 catalyzes nonoxi-

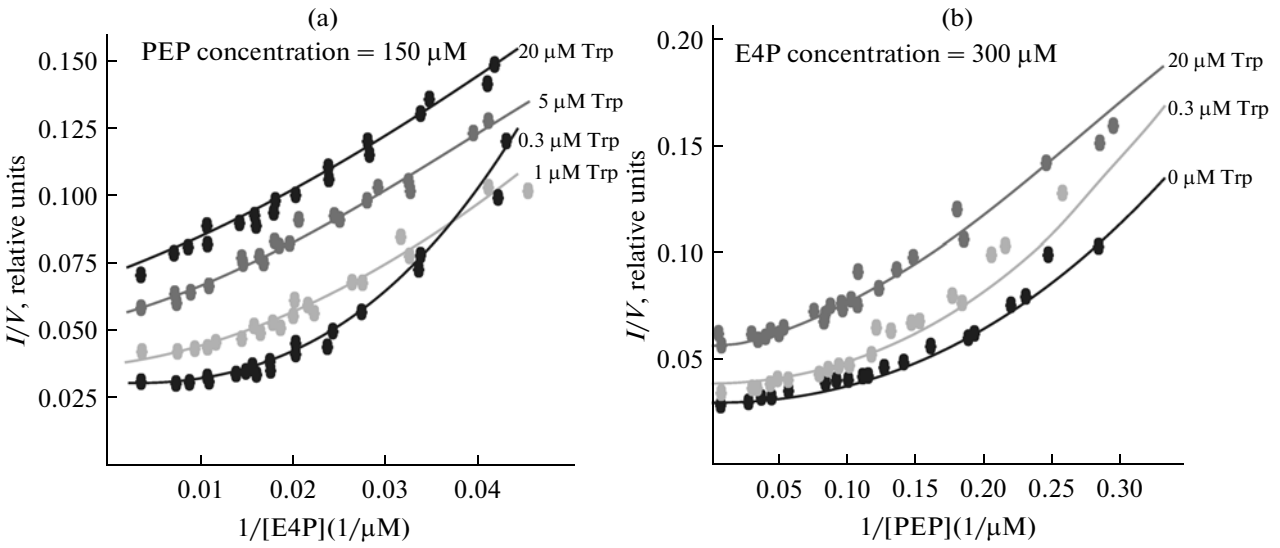

Fig. 1. The effects of various tryptophan concentrations on the rate of the enzymatic reaction catalyzed by DAHPS(Trp). The abscissa shows the inverse substrate concentration and the ordinate shows the inverse reaction rate. Dots show the experimental data [84] and curves show computations according to model (1) with the following parameter values: $k_f = 20.6\ s^{-1}$, $K_{m,S_1} = 35\ \mu M$, $K_{m,S_2} = 5.3\ \mu M$, $h_{S_1} = 2.6$, $h_{S_2} = 2.2$, $K_{iP_1} = 1\ mM$, $kI_{R,V_{max}} = 1.7$, $k_{R,V_{max}} = 5\ \mu M$, $kI_{R,K_{mS_1}} = 0.85$, $k_{R,K_{mS_1}} = 25\ \mu M$, $h_{R,K_{mS_1}} = 0.6$, $kI_{R,h_{S_1}} = 1.1$, $k_{R,h_{S_1}} = 1\ \mu M$, $k_{R,h_{S_1}} = 1$, $kI_{R,h_{S_2}} = 0.47$, $k_{R,h_{S_2}} = 1\ \mu M$, and $h_{R,h_{S_2}} = 2$.

dative cleavage of pyruvate into acetyl-CoA and formate. LDHA is constantly present in the cell; however, the concentration of this enzyme at low pH values increases tenfold [86]. Pyruvate also induces a two- to fourfold increase in the expression level of the *ldhA* gene and has a positive effect on the activity of this enzyme. Use of the method of generalized Hill functions for constructing a mathematical model for pyruvate metabolism in the *E. coli* cell can be illustrated by regulation of LDHA. As mentioned above, this enzyme catalyzes the reversible transformation of pyruvate (Pyr) into lactate (Lac) according to the following equation: Pyr + NAD(P)H ⟶ NAD(P) + Lac. Positive regulators of LDHA activity are Pyr and α-ketobutyrate (AKB) and negative regulators are ATP, oxamate (Ox), and the binary complex Pyr–NAD(P)H. Using GHFs, we have constructed model (3), which describes the dependence of enzymatic reaction rate on concentrations of the regulators AKB, Ox, and ATP and the substrates Pyr and NAD(P)H:

$$V = e_0 k_f \frac{(1 + \mathrm{Ox}/K_{1,\mathrm{OX}})}{(1 + \mathrm{Ox}/K_{2,\mathrm{OX}})} \times \frac{(1 + \mathrm{NADPH}/K_{1,\mathrm{nadph}})(\mathrm{NADPH}/K_{\mathrm{nadph}})}{(1 + \mathrm{NADPH}/K_{2,\mathrm{nadph}})(1 + \mathrm{NADPH}/K_{\mathrm{nadph}})} \times \frac{(\mathrm{PYR}/K_{\mathrm{pyr}})^{h_p}}{(1 + (\mathrm{PYR}/K_{\mathrm{pyr}})^{h_p})}, \quad (3)$$

where

$$h_p = n_p \frac{1 + \mathrm{AKB}/K_{1,\mathrm{akb}}}{1 + \mathrm{AKB}/K_{2,\mathrm{akb}}};$$

$$K_{\mathrm{pyr}} = Km_{\mathrm{pyr}}\left(\frac{1 + \mathrm{AKB}/K_{3,\mathrm{akb}}}{1 + \mathrm{AKB}/K_{4,\mathrm{akb}}}\right);$$

$$K_{\mathrm{nadph}} = Km_{\mathrm{nadph}} \frac{(1 + \mathrm{PYR}/K_{1,\mathrm{pyr}})(1 + \mathrm{ATP}/K_{1,\mathrm{atp}})}{(1 + \mathrm{PYR}/K_{2,\mathrm{pyr}})(1 + \mathrm{ATP}/K_{2,\mathrm{atp}})},$$

where e_0 is LDHA concentration; Pyr and NADHP are concentrations of the substrates pyruvate and NADPH; and Ox, AKB, and ATP are concentrations of the corresponding low-molecular-weight regulators. The values for the constants in model (3) were selected taking into account the experimental data shown in Fig. 3.

The described regulatory effects are of an intricate nonlinear character. Generalized efficiency constants (K_{nadph} and K_{pyr}) and the Hill nonlinearity constant h_p are functions of concentrations of AKB, Pyr, and ATP. For example, in the absence of AKB in the medium, h_p has the maximal value of 2, decreases upon the addition of AKB to the medium, and $h_p \approx 1.35$ at AKB = 20 mM.

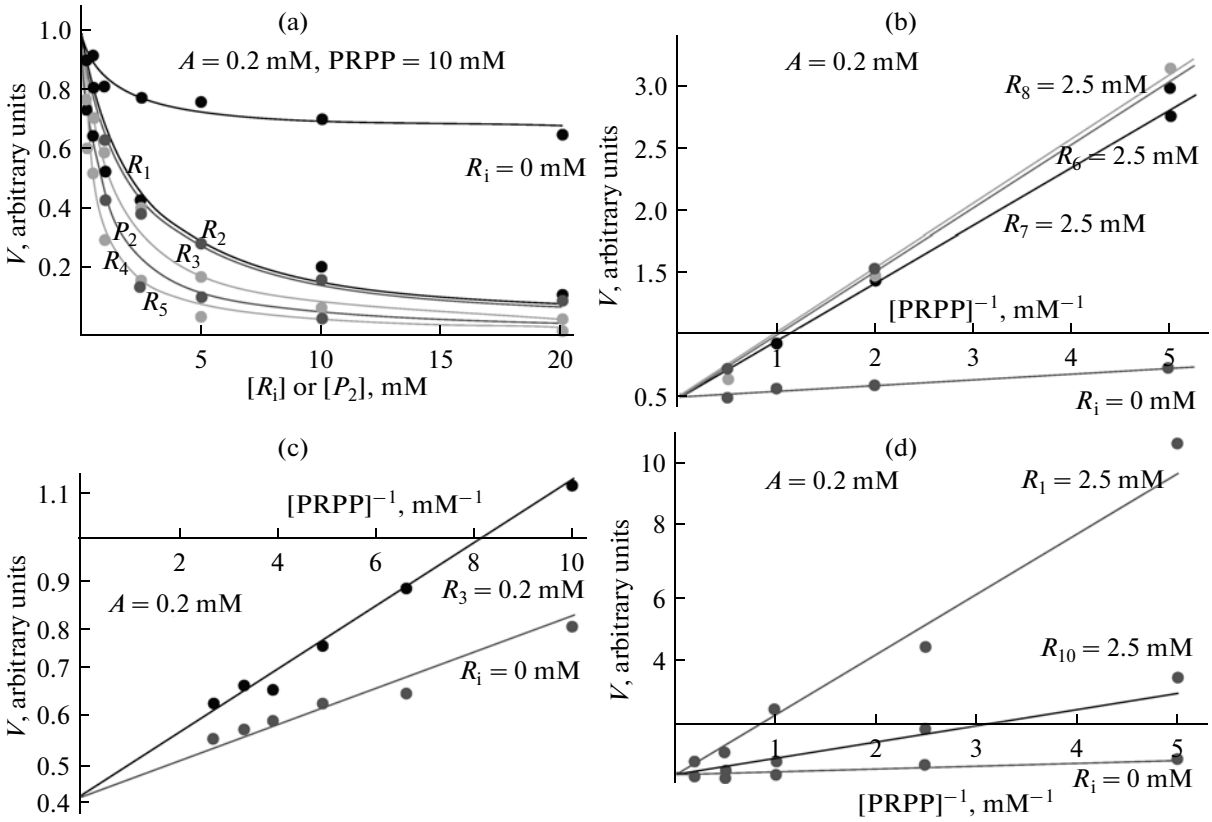

Fig. 2. The effects of (a) various regulators R_i and (b–d) PRPP on the rate of enzymatic reaction (V) catalyzed by APRT at various concentrations of the regulators R_i (for each calculated curve, $R_j = 0$ mM at $j \neq i$) and $A = 0.2$ mM. The dots on the plot are experimental data from [85]; the curves were computed using model (2) with the following parameter values: $k_{cat} = 560$ min^{-1}, $K_{m,S_1} = 0.011$ mM, $K_{m,S_2} = 0.1$ mM, $K_{i,P_1} = 0.8$ mM, $K_{i,P_2} = 0.03$ mM, $k_{i,R_1,S_2} = 0.13$ mM, $k_{i,R_2,S_2} = 0.02$ mM, $k_{i,R_3,S_2} = 0.27$ mM, $k_{i,R_4,S_2} = 0.008$ mM, $k_{i,R_5,S_2} = 0.0055$ mM, $k_{i,R_6,S_2} = 0.79$ mM, $k_{i,R_7,S_2} = 0.84$ mM, $k_{i,R_8,S_2} = 0.8$ mM, $k_{i,R_9,S_2} = 0.27$ mM, $k_{i,R_{10},S_2} = 0.27$ mM, $k_{i,R_{11},S_2} = 10$ mM, $k_{R_{12}} = 1.7$ mM, and $k_{IR_{12}} = 0.5$.

MATHEMATICAL MODELS FOR REGULATION OF EXPRESSION EFFICIENCY OF *E. coli* GENES

Expression Regulation of pyrC Gene

Expression of *pyrC* gene, encoding dihydroorotase, an enzyme involved in pyrimidine biosynthesis, is downregulated by pyrimidines [88]. Expression inhibition of this gene requires the formation of a hairpin at the 5'-end of *pyrC* transcript, which overlaps with the ribosome binding site. The hairpin formation is controlled via a nucleotide-sensitive selection of the *pyrC* transcription initiation. At a high CTP concentration, the main part of *pyrC* transcripts is initiated from nucleotide C17, located at a distance of 17 nucleotides from the *pyrC* translation start site. Such transcripts are able to form a stable hairpin at the 5'-end of mRNA in the region of ribosome binding site, thereby interfering with a normal translation initiation. At a low CTP and high GTP concentrations, the main part of the *pyrC* transcripts is initiated from nucleotide G15, which is by two nucleotides closer to the initiation codon as compared with C17. Consequently, the synthesized transcript is by two nucleotides shorter and is unable to form a stable hairpin at the 5'-end of mRNA, which provides for a normal translation initiation.

A uniqueness of this locus is in that biosynthesis of the protein PyrC is regulated via negative feedback by selection of the transcription start site, which influences the possibility of translation initiation of the transcribed mRNA. In the case of excess pyrimidines, the predominantly synthesized transcripts form a hairpin at the ribosome binding site, which blocks the translation initiation. In the case of pyrimidine deficiency in the cell, truncated transcripts are synthesized, which can be translated, thereby elevating the concentration of dihydroorotase in the cell.

A detailed biochemical scheme for genetic regulation of *pyrC* gene expression deducible from the information briefed above is exclusively intricate. However,

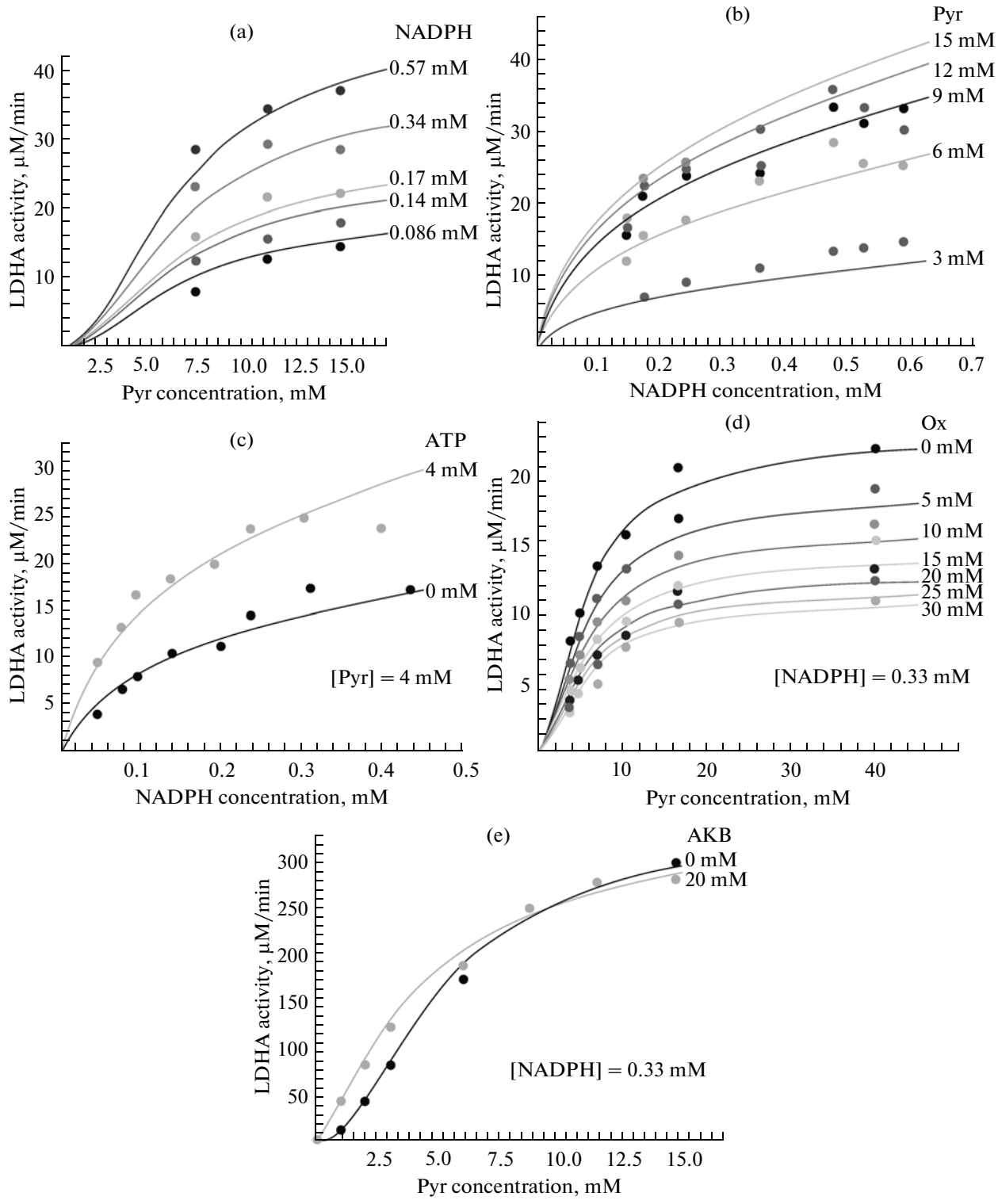

Fig. 3. Dynamics of LDHA activity depending on pyruvate concentration at various concentrations of (a) NADPH, (d) Ox, and (e) AKB and depending on NADPH concentration (b) at various pyruvate concentrations and (c) in the presence or absence of ATP. The ordinate shows the enzyme activity (in micromoles of NADPH oxidized over 1 min at pH 7.5). The dots on plots are experimental data from [86]; the curves were computed using model (3) with the following parameter values: $k_j = 566\ s^{-1}$, $Km_{pyr} = 4.2$ mM, $Km_{hadph} = 40$ mM, $K_{1,\,pyr} = 8$ mM, $K_{2,\,pyr} = 4$ mM, $K_{1,\,nadph} = 1$ mM, $K_{2,\,nadph} = 0.083$ mM, $K_{1,\,ox} = 100$ mM, $K_{2,\,ox} = 17.65$ mM, $K_{1,\,atp} = 1$ mM, $K_{2,\,atp} = 0.513$ mM, $K_{1,\,akb} = 1$ mM, $K_{2,\,akb} = 0.667$ mM, $K_{3,\,akb} = 1$ mM, $K_{4,\,akb} = 0.667$ mM, and $h_p = 2$.

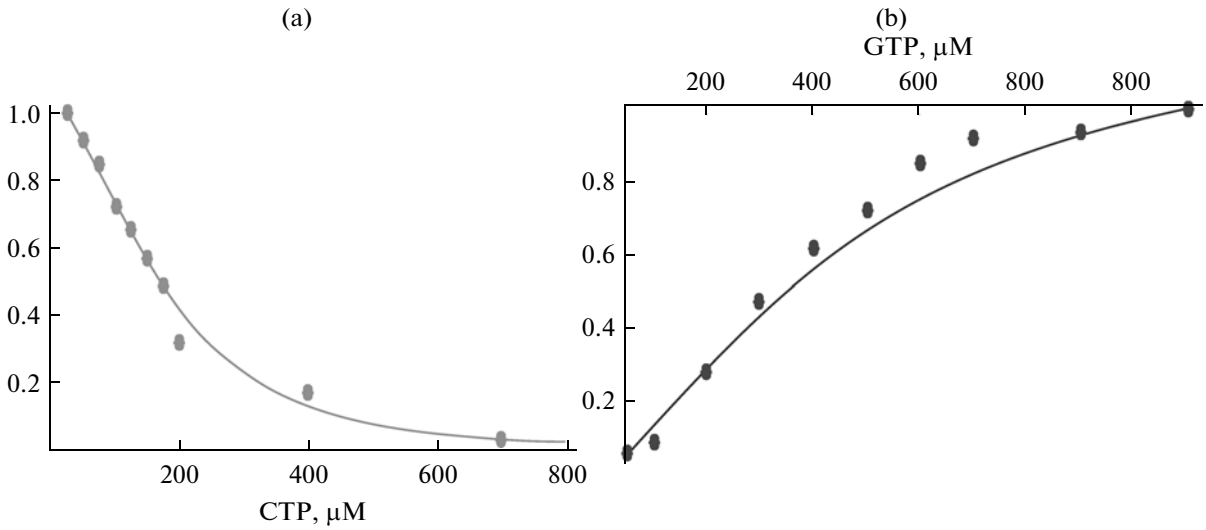

Fig. 4. The effects of (a) CTP and (b) GTP concentrations on formation of translatable mRNA transcripts encoding the protein PyrC in the presence of (a) 1.1 mM GTP, 2.7 mM ATP and (b) 0.1 mM CTP. The ordinate shows the fraction of translated transcripts relative to the maximal amount; the maximal amount in the case of (a) CTP variation is the value obtained for GTP = 1.1 mM and CTP = 25 μM and in the case of (b) GTP variation it is at GTP = 1.1 mM and CTP = 100 μM. The dots in the plots are the experimental data from [88]; the curves were computed using model (4) with the following parameter values: $k_{GTP} = 48$ μM, $k_{CTP} = 11$ μM, $\omega = 0.002$, $n_c = 2.8$, and $n_g = 1.3$.

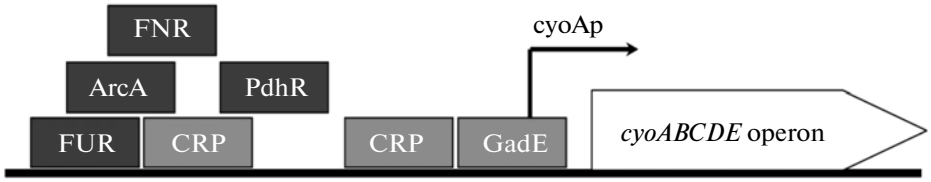

Fig. 5. Probable structure of cyoAp promoter in *cyoABCDE* operon, encoding cytochrome *b* oxidase; FNR, ArcA, PdhR, and FUR are transcription inhibitors; CRP and GadE are transcription activators (according to http://biocyc.org/ECOLI).

the GHF gives a very compact description of the processes in question:

$$V = V_{\max}\frac{\left(\frac{GTP}{k_{GTP}}\right)^{n_g}}{1+\left(\frac{GTP}{k_{GTP}}\right)^{n_g}+\left(\frac{CTP}{k_{CTP}}\right)^{n_c}+\omega\left(\frac{GTP}{k_{GTP}}\right)^{n_g}\left(\frac{CTP}{k_{CTP}}\right)^{n_c}}, \quad (4)$$

where V and $V_{\max}$ are the current and maximal rates of synthesis of the active mRNA, which can be involved in an active synthesis of protein PyrC, respectively; *GTP* and *CTP* are concentrations of GTP and CTP; k_{GTP} and k_{CTP} are the constants of effective influence of GTP and CTP on mRNA synthesis, respectively; ω is the efficiency constant of joint GTP and CTP effect on mRNA synthesis; and n_g and n_c are the constants characterizing the degree of nonlinearity of the effects of GTP and CTP on mRNA synthesis. The results of theoretical computations according to model (4) and the corresponding experimental data are shown in Fig. 4.

Note that model (4) with its relative simplicity (as compared with the complexity of the considered molecular biological processes) yet provides for a good agreement between the experimental data and computation results. Moreover, it follows from the model that transcription factors have, although weakened, yet significant joint effect on the promoter (with a value of ω considerably lower than unity but still nonzero).

Expression Regulation of cyoABCDE Operon (an Example of Equation Derivation)

Transfer of *E. coli* cells into the medium saturated with oxygen considerably upregulates the expression of the *cyoABCDE* operon, encoding cytochrome *b* oxidase. A scheme for the structure–function organization of the promoter region in this operon is shown in Fig. 5. The factor GadE, is this case, plays the role of an activator [89]; under anaerobic or microaerobic conditions, the action of this factor is suppressed by the competing transcription regulators FNR and ArcA, which repress the expression of *cyoABCDE* operon [90–92]. In

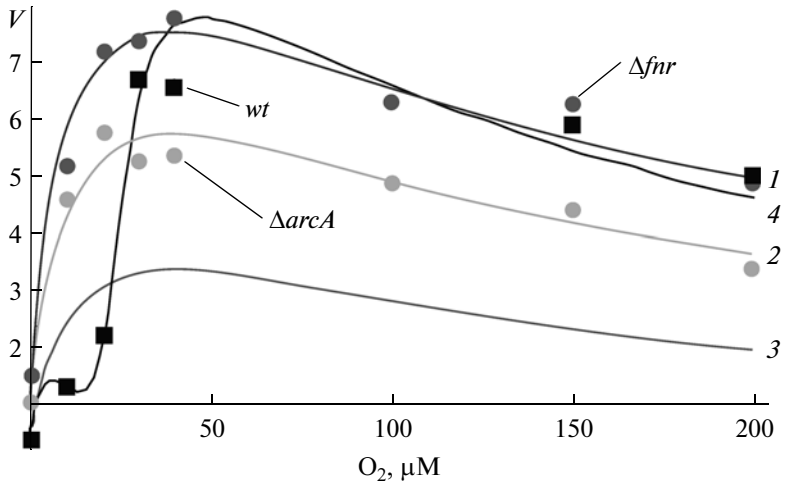

Fig. 6. Dependence of the transcriptions level of *cyoABCDE* operon on oxygen concentration in the medium for wild-type (*wt*) *E. coli* cells and mutant strains Δ*arcA* and Δ*fnr*; dots in the plots are experimental data from [94] and solid lines show the computation results using model (12) (see below): (*1*) $V_{\Delta fnr}$; (*2*) $V_{\Delta arcA}$; and (*3*) V_{wt}; and model (16): (*4*) V_{wt}. the parameter values used for calculating theoretical curves are $k_{v1} = 0.036$, $k_{v2} = 0.024$, $k_{v3} = 0.040$, $h_{v1} = 1$, $h_{v2} = 4.9$, $\omega = 0.053$, $v_{ini} = 30$, $dA = 19$, $dF = 27$, $ka_1 = kf_1 = 23$, $ka_2 = kf_2 = 4.5$, $h_{a1} = h_{f1} = 2$, and $h_{a2} = h_{fa} = 1.5$.

this process, a mediated FNR action via the activation of ArcA factor is observed [93].

Based on the mechanisms assumed for transcription factors, it is possible to propose a minimal biochemical scheme for the action of transcription factors on the expression efficiency of *cyoABCDE* operon. However, the direct data for selection of optimal parameter values for the model are insufficient and not shown. On the other hand, the kinetics of changes in the activity of this promoter, depending on the oxygen concentration in the medium, has been studied (Fig. 6), which makes it possible to construct a model that directly relates the activity of *cyoABCDE* promoter with the oxygen concentration in the cell. The model will be constructed in terms of GHFs. When deriving equations, take into account that oxygen directly changes the activity of FNR and ArcA factors. Assume that the concentrations of the remaining factors are constant and are not considered.

Designate the concentrations of ArcA and FNR factors under anaerobic conditions as *cA* and *cF*, respectively. The concentrations of active repressor species depending on oxygen concentration is described by GHFs as

$$cAo(s) = cA\frac{1+\left(\frac{s}{ka_1}\right)^{h_{a1}}}{1+\left(\frac{s}{ka_2}\right)^{h_{a2}}} \quad (5)$$

and

$$cFo(s) = cF\frac{1+\left(\frac{s}{kf_1}\right)^{h_{f1}}}{1+\left(\frac{s}{kf_2}\right)^{h_{f2}}}. \quad (6)$$

Taking into account the mutual arrangement of the binding sites for factors ArcA and FNR in the cyoA promoter (see Fig. 5), the fraction of active promoters depends on the oxygen concentration as

$$G_{cyo,\,wt}(s) = \frac{1}{1+\frac{cAo(s)}{kpa}+\frac{cFo(s)}{kpf}+\omega\frac{cAo(s)}{kpa}\frac{cFo(s)}{kpf}}, \quad (7)$$

where $G_{cyo,\,wt}(s)$ is the fraction of active CyoA promoters; s is the oxygen concentration in medium; and the meaning of the remaining parameters and their dimensionalities are easily understandable from equations and are not detailed.

Excluding from Eq. (7) the components that describe the effect of oxygen via ArcA (FNR), we get the equation for the fraction of active promoters for mutants Δ*arcA*(Δ*fnr*):

$$G_{cyo,\,\Delta arcA}(s) = \frac{1}{1+\frac{cFo(s)}{kpf}}, \quad (8)$$

and

$$G_{cyo,\,\Delta fnr}(s) = \frac{1}{1+\frac{cAo(s)}{kpa}}. \quad (9)$$

Using Eqs. (7)–(9), we get the following equation for determining the activity of promoters:

$$V_{wt}(s) = \nu_{\exp} G_{cyo,\,wt}(s), \quad V_{\Delta fnr}(s) = \nu_{\exp} G_{\Delta fnr}(s), \quad V_{\Delta arcA}(s) = \nu_{\exp} G_{\Delta arcA}(s).$$

First assess the parameter values for models (8) and (9). Note here that Eqs. (8) and (9) contain the relations $dA = cA/kpa$ and $dF = cF/kpf$. For clearness, we put down the equations for $V_{\Delta fnr}(s)$ and $V_{\Delta arcA}(s)$ taking into account (5), (6), (8), and (9):

$$V_{\Delta fnr}(s) = \nu_{ini} \frac{1}{1 + \left(\frac{s}{ka_1}\right)^{h_{a1}}} \Big/ \left(1 + dA \frac{1}{1 + \left(\frac{s}{ka_2}\right)^{h_{a2}}}\right) \quad (10)$$

and

$$V_{\Delta arcA}(s) = \nu_{ini} \frac{1}{1 + \left(\frac{s}{kf_1}\right)^{h_{f1}}} \Big/ \left(1 + dF \frac{1}{1 + \left(\frac{s}{kf_2}\right)^{h_{f2}}}\right). \quad (11)$$

The values for parameters ν_{ini}, dA, ka_1, ka_2, h_{a1}, h_{a2}, dF, kf_1, kf_2, h_{f1}, and h_{f2} are selected based on the experimental data shown in Fig. 6 as dots. Based on these values, we get at a zero oxygen concentration that $V_{\Delta arcA}(0) = \nu_{ini} \frac{1}{1 + dA} = 1.2$ and $V_{\Delta fnr}(0) = \nu_{ini} \frac{1}{1 + dF} = 1.5$, which makes it possible to assess two parameters via the third one. Note also that the activity of promoters rapidly increases approximately four- to sixfold with the growth in oxygen concentration from 0 to 40 mM and then slowly decreases (see Fig. 6). This suggests a qualitative conclusion that the concentrations of active species of ArcA and FNR repressors initially decrease severalfold and then slowly grow. These data suggest that the following conditions should be met: $ka_1 > ka_2$, $h_{a1} > h_{a2}$, $kf_1 > kf_2$, and $h_{f1} > h_{f2}$. Indeed, these conditions provide for the prevalence of activity inhibition for repressors ArcA and FNR at low oxygen concentrations and prevalent restoration of their high activity level at high oxygen concentrations. Note that here we do not solve the problem of reconstruction of the mechanisms providing for regulation of ArcA and FNR activities depending on the oxygen concentration in medium. We only state that the phenomenon of restoration of high concentrations of active repressor (ArcA and FNR) species at high oxygen concentrations should be present in the system, because otherwise it is impossible to explain the available kinetic data. This restoration effect can be determined by an increase in the rate of synthesis of these repressors at a high oxygen level, increase in their stability, or both processes. However, other factors can also contribute to this phenomenon.

Turning back to the estimation of parameter values, computation gives the following values: $\nu_{ini} = 30$, $dA = 19$, $dF = 27$, $ka_1 = kf_1 = 23$, $ka_2 = kf_2 = 4.5$, $h_{a1} = h_{f1} = 2$, and $h_{a2} = h_{f2} = 1.5$. A remarkable biologically significant property of this parameter set is that the kinetic characteristics of pcyoABCDE promoter in the mutants Δ*arcA* and Δ*fnr* are describable by structurally and parametrically identical models (8) and (9) for the change in concentration of active repressor (ArcA and FNR) species depending on oxygen concentration. The only exclusion is the values for parameters *dA* and *dF*, which demonstrate the difference in the concentrations of active repressor species initially present in mutant cells and(or) different effects caused by these repressors on promoter, or both effects simultaneously.

Now turn to the approximation of promoter activities in the native cell, carrying normal *arcA* and *fnr* genes. In general, the concentrations of ArcA and FNR repressors in this cell type can differ from the corresponding concentrations in the mutants Δ*arcA* and Δ*fnr*. In other words, we can, in principle, consider that the parameters in native cell differ from the values for the mutant cells. Following the principle of simplicity, assume that the values of the parameters for models (10) and (11) can be, without any change, transferred to the model intended for describing the activity of pcyoABCDE promoter in the native cell. Consider model (7), taking which into account we determine the promoter activity as

$$V_{wt}(s) = \nu_{ini} G_{cyo,\,wt}(s). \quad (12)$$

This equation has only one degree of freedom, the parameter ω; the values of all the remaining parameters were estimated above when adapting models (9) and (10). The value of parameter ω is easily computable based on the zero point of the curve describing the experimentally measured activity kinetics for the promoter in *cyoABCDE* operon (Fig. 6):

$$V_{wt}(0) = \nu_{ini} \frac{1}{1 + dA + dF + \omega(dA dF)} = 0.4.$$

This gives the result that $\omega = 0.053$. Comparison of the calculation for function $V_{wt}(s) = \nu_{ini} G_{cyo,\,wt}(s)$ with the corresponding experimental data (Fig. 6) reveals several fundamental discrepancies, namely, a later amplification of promoter activity as obtained from the model, and a lower maximal level of its activity as compared with the experimentally observed data. Therefore, model (12) requires further modification.

Here, two problems are to be solved: first, to take into account the presence of a lag period in promoter activation and, second, to elevate the final maximal amplification to the level observed in the experiment. The data that FNR protein can act as an activator of *ArcA* gene expression hint at a possible direction of model modification. Existence of such mechanism

Table 1. Values of the parameter *dA* as a function of oxygen concentration in the medium

O_2, μM	0	10	20	30	40	100	150	200
dA	19.4	56.2	37.2	−4.3	−3.6	−5.6	−6.9	−6.0

Table 2. Values of the parameter V_{ini} as a function of oxygen concentration in the medium

O_2, μM	0	10	20	30	40	100	150	200
V_{ini}	29.7	16.2	21.6	60.9	58.8	67.5	76.2	76.2

was experimentally demonstrated [95]. The attempt to take this fact into account entails the need in description of the parameter *dA* as a function of concentration of a certain FNR species that depends on oxygen concentration. The behavior of this function depending on oxygen concentration is easily calculable using functions (7), (10), and (11), the estimated parameter values, and experimental data (see Fig. 6). Thus, we get a series (Table 1) demonstrating an approximate form of the parameter *dA* as a function of oxygen concentration in the medium.

The data listed in Table 1 suggest that the mechanism of *ArcA* gene activation by FNR protein fails to describe experimental data at an oxygen concentration in the medium exceeding 30 μM, because the values of oxygen concentration cannot be negative. We have no other hypotheses that can be proposed based on experimental data. Therefore, let us use the possibilities provided by GHFs. In principle, this class of functions provides for constructing approximations of kinetic processes without taking into account the structural features of the considered object. We modify model (12) so that it would reduce to models (10) and (11) when simulating mutations Δ*fnr* and Δ*arcA*. Assume that the parameter ν_{ini} is a function of the product of concentrations of oxygen species of the repressors ArcA, *Ao*(*s*), and FNR, *Fo*(*s*):

$$V_{ini}(s) = \nu_{ini}\frac{1+(Ao(s)Fo(s)/k_{\nu 1}^2)^{h_{\nu 1}}}{1+(Ao(s)Fo(s)/k_{\nu 2}^2)^{h_{\nu 2}}+(Ao(s)Fo(s)/k_{\nu 3}^2)^{h_{\nu 1}}}. \quad (13)$$

The following functions are used for describing the effect of oxygen on repressor activity:

$$Ao(s) = cA\frac{\left(\frac{s}{ka_1}\right)^{h_{a1}}}{1+\left(\frac{s}{ka_2}\right)^{h_{a2}}} \quad (14)$$

and

$$Fo(s) = cF\frac{\left(\frac{s}{kf_1}\right)^{h_{f1}}}{1+\left(\frac{s}{kf_2}\right)^{h_{f2}}}, \quad (15)$$

which are subfunctions of functions (5) and (6), respectively. The behavior of function (13) can be also derived from the kinetic data shown in Fig. 6 (Table 2).

Using data from Table 2, we estimate the parameters $k_{\nu 1} = 0.036$, $k_{\nu 2} = 0.024$, $k_{\nu 3} = 0.040$, and $h_{\nu 1} = 1$, $h_{\nu 2} = 4.9$ for function (13) and obtain the following model:

$$V(s) = V_{ini}(s)G_{cyo,\,wt}(s), \quad (16)$$

which describes the corresponding experimental data (Fig. 6, curve *4*).

The above described models are part of the database on elementary models of enzymatic reactions and genetic elements, which, as is mentioned above, contain 370 elementary models [79]. Such a database will allow a wide range of in silico experiments to be conducted—from modeling of small local molecular genetic systems controlling individual metabolic pathways to construction of models for global molecular genetic systems, including the system controlling the overall *E. coli* cell metabolism, and will make it possible to solve target basic and applied problems in metabolic engineering. Find below an example of using the database of elementary models in construction of the model for pyrimidine biosynthesis.

A Mathematical Model for the Metabolic Pathway of Pyrimidine Biosynthesis

The metabolic pathway of UTP and CTP biosynthesis is shown in Fig. 7. It comprises nine successive stages performed by the enzymes carbamoyl phosphate synthetase (E1, CPSase), aspartate transcarbamoylase (E2, ATCase), dihydroorotase (E3, DHOase), dihydroorotate dehydrogenase (E4, DHODase), orotate phosphoribosyltransferase (E5, OPTase), orotidine monophosphate

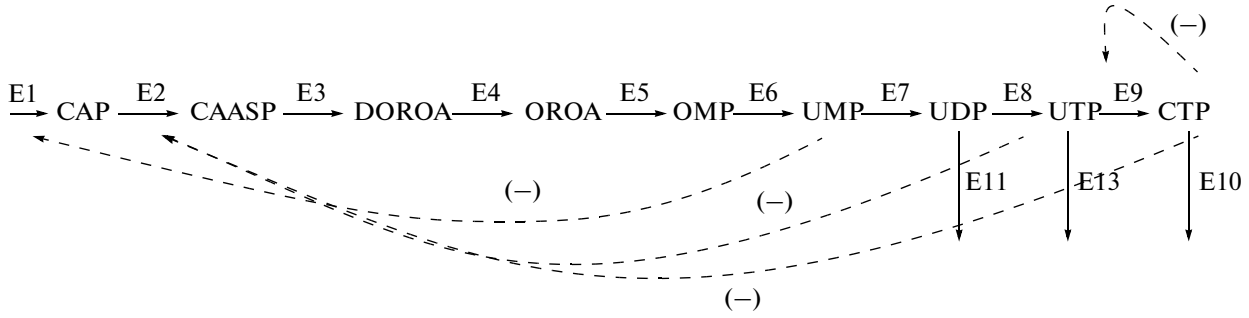

Fig. 7. Scheme of successive reactions in biosyntheses of the nucleotides UTP and CTP in *E. coli* cells; dashed arrows show an allosteric inhibition of the enzymes CPSase (E1), ATCase (E2), and CTPase (E9), which catalyze production of carbamoyl phosphate (CAP), carbamoyl aspartate (CAASP), and UTP amination to CTP, respectively.

decarboxylase (E6, OMPase), uridine monophosphate kinase (E7, UMP kinase), nucleoside diphosphate kinase (E8, NDK), and cytidine triphosphate synthetase (E9, CTPase), respectively. Three enzymatic reactions from this sequence (E1, E2, and E9) are subject to allosteric regulation by uridine triphosphate (UTP) and cytidine triphosphate (CTP), namely, production of carbamoyl phosphate (CAP) and carbamoyl aspartate (CAASP) and UTP amination to CTP. The transformations of uridine diphosphate (UDP) into deoxyuridine diphosphate (dUDP), UTP into deoxyuridine triphosphate (dUTP), and CTP into deoxycytidine triphosphate (dCTP) are catalyzed by the enzymes ribonucleoside diphosphate reductase (E11, RDREDase) and ribonucleoside triphosphate reductase (E13 and E10, RNTPRase), respectively.

The mathematical model of pyrimidine synthesis is assembled based on the elementary models of the corresponding enzymatic reactions involved in the biosynthesis of the ribonucleoside phosphates UTP and CTP in the *E. coli* cell [79]:

$$\begin{cases} \frac{dx1}{dt} = V_1 - V_2, \\ \frac{dx2}{dt} = V_2 - V_3, \\ \frac{dx3}{dt} = V_3 - V_4, \\ \frac{dx4}{dt} = V_4 - V_5, \\ \frac{dx5}{dt} = V_5 - V_6, \\ \frac{dx6}{dt} = V_6 - V_7, \\ \frac{dx7}{dt} = V_7 - V_8 - V_{11}, \\ \frac{dx8}{dt} = V_8 - V_9 - V_{12}, \\ \frac{dx9}{dt} = V_9 - V_{10}, \end{cases} \quad \text{where} \quad \begin{cases} V_1 = \frac{\nu x1}{1 + \frac{x6}{km1}}, \quad V_2 = \frac{\nu x2 \cdot x1}{km2 + x1} \frac{1 + \left(\frac{x9}{k21}\right)^{h21}}{1 + \left(\frac{x9}{k22}\right)^{h22}} \frac{1}{1 + \frac{x8}{ku2}}, \\ V_3 = \frac{\nu x3 \cdot x2}{km3 + x2}, \quad V_4 = \frac{\nu x4 \cdot x3}{km4 + x3}, \quad V_5 = \frac{\nu x5 \cdot x4}{km5 + x4}, \quad V_6 = \frac{\nu x6 \cdot x5}{km6 + x5}, \\ V_7 = \frac{\nu x7 \cdot x6}{km7 + x6} \frac{1}{1 + \left(\frac{x8}{ku7}\right)^{hu7}}, \quad V_8 = \frac{\nu x8 \cdot x7}{km8 + x7}, \quad V_9 = \frac{\nu x9 \left(\frac{x8}{ku9}\right)^{hu9}}{1 + \left(\frac{x8}{ku9}\right)^{hu9}}, \\ V_{10} = \frac{kd1 \frac{x9}{km10}}{kd2 + \frac{x9}{km10}} + kd6 \cdot x9, \quad V_{11} = \frac{kd3 \cdot x7}{km11 + x7}, \\ V_{12} = \frac{kd4 \frac{x8}{km12}}{kd2 + \frac{x8}{km12}} + kd5 \cdot x8. \end{cases} \tag{17}$$

The concentrations $x_1, \ldots, x_8, x_9$ of the low-molecular-weight compounds CAP, ... UTP, CTP in the order shown in Fig. 7, respectively, are the variables in this model.

In the case of an optimal set of parameter values that we selected via a numeric adaptation to published data [97–107], the model functions in a continuous oscillation mode (Fig. 8).

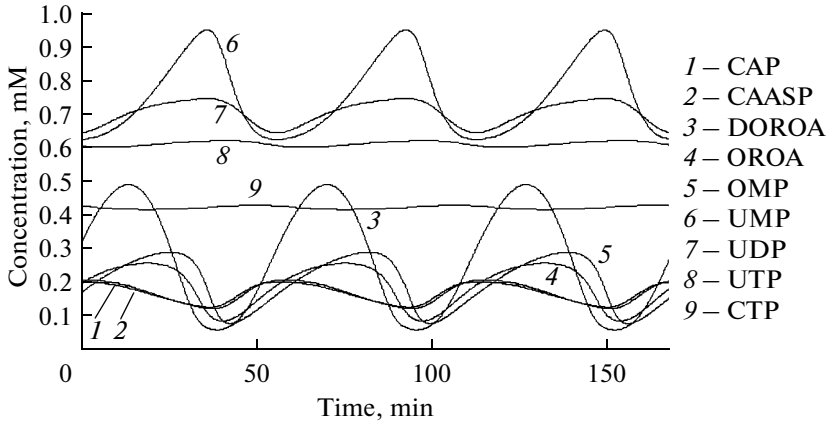

Fig. 8. Dynamics of oscillations of concentrations of ribopyrimidine nucleotides and their precursors computed using model (17) with the following parameter values: $\nu x1 = 0.057$ mM/s, $km1 = 0.05$ mM, $\nu x2 = 0.058$ mM/s, $km2 = 0.92$ mM, $k21 = 0.036$ mM, $k22 = 0.02$ mM, $h21 = 1.35$, $h22 = 1.39$, $ku2 = 30$ mM, $\nu x3 = 0.014$ mM/s, $km3 = 0.47$ mM, $\nu x4 = 0.004$ mM/s, $km4 = 0.027$ mM, $\nu x5 = 0.0033$ mM/s, $km5 = 0.04$ mM, $\nu x6 = 0.0044$ mM/s, $km6 = 0.006$ mM, $\nu x7 = 4.11$ mM/s, $km7 = 0.17$ mM, $ku7 = 0.04$ mM, $hu7 = 2.5$, $\nu x8 = 0.0036$ mM/s, $km8 = 0.09$ mM, $\nu x9 = 0.003$ mM/s, $ku9 = 0.3$ mM, $hu9 = 1.5$, $kd1 = 0.0023$ mM/s, $km10 = 4$ mM, $kd2 = 0.011$ mM/s, $kd6 = 0.0003$ l/s, $kd3 = 0.0006$ mM/s, $km11 = 0.25$ mM, $kd4 = 0.0009$ mM/s, $kd5 = 0.00019$ l/s, and $km12 = 4$ mM.

The oscillation period for concentrations of metabolites in this subsystem is approximately 50 min. A large oscillation amplitude as compared with the mean concentration is observed for CAP, CAASP, dihydroorotate (DOROA), orotate (OROA), orotidine monophosphate (OMP), UMP, and UDP; the deviation from the mean concentration during oscillation for UTP and CTP is less than 1%.

These results demonstrate that the description of kinetics of metabolic processes in the cell taking into account nonlinear effects in the regulatory mechanisms of metabolic networks leads to a model with continuous oscillations. We yet do not know (development of the corresponding model is still in progress) whether these oscillations will be retained if the model of this metabolic pathway will additionally take into account the nonlinear genetic processes providing for expression regulation of the genes encoding the corresponding enzymes and transcription factors. Using a particular model of expression regulation of the *cyoABCDE* operon, we demonstrated above a nonlinear character of the changes in its activity in response to change in the oxygen concentration in medium. This example shows that nonlinearity is a significant factor that modulates nontrivial function modes of biochemical and genetic systems and that this cannot be ignored when constructing the models of metabolic pathways functioning under conditions far from equilibrium.

CONCLUSIONS

Construction of the models for metabolic pathways that display a forecasting ability is a topical problem in metabolic engineering. If a mathematical model is developed in terms of differential equations, then the problem to be solved is to determine the form of the right-hand members of equations. Since enzymatic reactions and genetic processes of gene expression form the basis for the function of metabolic systems, the models can be constructed in two stages. At the first stage, models are constructed for elementary subsystems of enzymatic reactions and genetic elements with subsequent development of large-scale models for metabolic pathways. Completeness of the models for elementary subsystems depends on the available knowledge about their structural and dynamic characteristics. If a subsystem has been studied in sufficient detail, it is possible to construct a comprehensive biochemical model to use it further as an elementary model. The modeling route from a biochemical scheme to a system of differential equations is the most advantageous. However, it is hardly feasible for the majority of real subsystems, because their biochemical mechanisms are studied in insufficient detail. In this case, there is no choice but to construct approximate models, which at the elementary level correspond in their complexity to the available data on the functioning of subsystems and at the level of a large-scale model provide for solving the stated target problems. The limit case for a simplified description of elementary subsystems is a complete neglect of the mechanisms underlying the function of subsystems. This approach is used in flux balance models of metabolic pathways and gives linear systems of ordinary differential equations. This makes it possible to construct flux balance models of large dimensionalities, which enhance prediction of the levels of metabolites, including technologically significant dependences on the initial conditions, as well as their optimization [30, 33, 43, 52].

However, flux models are applicable only to the cases when a target biological system is in a quasi-stationary state relative to the fluxes of metabolites. This

is a rather strong limitation, which is not generally met in the case of living cells [107–109]. The briefed results on analysis of a particular mathematical model (17), describing the function of a fragment of the metabolic system yielding pyrimidines, also demonstrate a limited field of applicability for linear flux models. This model is constructed taking into account the nonlinear effects resulting from an allosteric regulation of several enzymes by the products of synthesis and, as has been shown, functions in the mode of continuous oscillations. Presumably, it is necessary to discard the assumption of a global quasi-stationarity of metabolic systems to increase the forecasting capacity of the developed models. For this purpose, we propose to supplement flux models with nonlinear terms describing the rates of enzymatic reactions as well as with the models describing expression regulation of the genes encoding enzymes, their subunits, and other proteins, for example, transcription factors, that play a key role in functioning of the corresponding subsystems. In the context of such an approach, the transition from linear flux models to nonlinear models can be stepwise via replacing the rates described by linear terms with nonlinear models only for the elementary subsystems with sufficient experimental kinetic data.

In large-scale models, we propose to take into account the nonlinear effects in terms of generalized Hill functions. In general, description of the rates of biochemical and genetic processes in terms of generalized Hill functions requires only sufficient kinetic data; however, the equation can be derived also taking into account the specific structure–function features of the considered subsystem (if available). Use of generalized Hill functions allows excess details in the elementary model under conditions of data deficiency to be avoided; on the other hand, this provides for an accurate description of the response dynamics of a subsystem to key parameters. This is important from the methodological standpoint, because it is sometimes much better when modeling metabolic systems far from equilibrium to use phenomenological nonlinear models of their subsystems than certainly inadequate linear approximations. We believe that application of generalized Hill functions as a tool for approximation of nonlinear biochemical and genetic processes will make it possible to develop large-scale mathematical models of metabolic systems in the case of insufficient data on the mechanisms underlying the function of individual subsystems so that these models will have forecasting ability under conditions far from equilibrium.

On the other hand, taking into account the current trends in the field of in silico metabolic engineering directed at large-scale mathematical modeling of target objects [38, 55, 56, 58] and simulation of their behavior dynamics in in silico experiments, the question arises on development of computer resources providing for such studies [31, 39, 59]. For this purpose, we have developed a computer resource that unites a database of models for a number of *E. coli* elementary subsystems [79] and the tools for construction of mathematical models for metabolic and molecular genetic systems functioning in the *E. coli* cell [110]. The tools within this resource provide for computation of qualitative and quantitative characteristics of the studied systems [111]. This computer resource makes it possible to construct and study the models for any processes composed of the models of both genetic and nongenetic elements described in the database. The potential of this resource as a tool for theoretical analysis of basic and applied issues on gene network dynamics is determined by the volume of the database compiling elementary models and will expand with further development of this database. All the above described models are integral components of the database on models with this computer resource and demonstrate the possibilities of generalized chemical kinetic approach to modeling of dynamic processes.

ACKNOWLEDGMENTS

The work was supported by the Russian Foundation for Basic Research (grant no. 08-04-01008), the Russian Academy of Sciences (projects nos. 22.8 and 21.26), the Presidium of the Siberian Branch of the Russian Academy of Sciences (project nos. 107 and 119), and the Program for the Support of Leading Scientific Schools (grant no. NSh-2447.2008.4).

REFERENCES

1. Bailey, J.E., *Science*, 1991, vol. 252, pp. 1668–1675.
2. Cameron, D.C. and Tong, I.T., *Appl. Biochem. Biotechnol.*, 1993, vol. 38, pp. 105–140.
3. Koffas, M., Roberge, C., Lee, K., and Stephanopoulos, G., *Annu. Rev. Biomed. Eng.,* 1999, vol. 1, pp. 535–557.
4. Stephanopoulos, G., *Metab. Eng.*, 1999, vol. 1, no. 1, pp. 1–11.
5. Harris, L.M., Desai, R.P., Welker, N.E., and Papoutsakis, E.T., *Biotechnol. Bioeng.*, 2000, vol. 67, pp. 1–11.
6. Barkovich, R. and Liao, J.C., *Metab. Eng.*, 2001, vol. 3, pp. 27–39.
7. Nielsen, J., *Appl. Microbiol. Biotechnol.*, 2001, vol. 55, pp. 263–283.
8. Thykaer, J. and Nielsen, J., *Metab. Eng.*, 2003, vol. 5, no. 1, pp. 56–69.
9. Leuchtenberger, W., Huthmacher, K., and Drauz, K., *Appl. Microbiol. Biotechnol.*, 2005, vol. 69, pp. 1–8.
10. Raab, R.M., Tyo, K., and Stephanopoulos, G., *Adv. Biochem. Eng. Biotechnol.*, 2005, vol. 100, pp. 1–17.
11. Ikeda, M., *Appl. Microbiol. Biotechnol.*, 2006, vol. 69, no. 6, pp. 615–626.
12. Wendisch, V.F., Bott, M., and Eikmanns, B.J., *Curr. Opin. Microbiol.,* 2006, vol. 9, pp. 268–274.
13. Kern, A., Tilley, E., Hunter, I.S., Legisa, M., and Glieder, A., *J. Biotechnol.,* 2007, vol. 129, pp. 6–29.

14. Sprenger, G.A., *Appl. Microbiol. Biotechnol.*, 2007, vol. 75, pp. 739–749.
15. Kim, T.Y., Sohn, S.B., Kim, H.U., and Lee, S.Y., *Biotechnol. J.*, 2008, vol. 3, pp. 612–623.
16. Nielsen, J., *J. Bacteriol.*, 2003, vol. 185, pp. 7031–7035.
17. Stephanopoulos, J., Alper, H., and Moxley, J., *Nat. Biotechnol.*, 2004, vol. 22, no. (10, pp. 1261–1267.
18. Bailey, J.E., *Biotechnol. Prog.*, 1998, vol. 14, pp. 8–20.
19. Hatzimanikatis, V. and Liao, J.C., *Biotechnol. Bioeng.*, 2002, vol. 79, pp. 504–508.
20. Domach, M.M., Leung, S.K., Cahn, R.E., Cocks, G.G., and Shuler, M.L., *Biotechnol. Bioeng.*, 1984, vol. 26, pp. 203–216.
21. Ataai, M.M. and Shuler, M.L., *Biotechnol. Bioeng.*, 1985, vol. 27, pp. 1027–1035.
22. Peretti, S.W. and Bailey, J.E., *Biotehcnol. Bioeng.,* 1986, vol. 28, no. 11, pp. 1672–1689.
23. Shu, J., and Shuler, L.M., *Biotechnol. Bioeng.,* 1989, vol. 33, no. 9, pp. 1117–1126.
24. Hatzimanikatis, V., Emmerling, M., Sauer, U., and Bailey, J.E., *Biotechnol. Bioeng.*, 1998, vol. 58, pp. 154–161.
25. Wiecheri, W., *J. Biotechnol.*, 2002, vol. 94, no. 1, pp. 37–63.
26. Gadkar, K.G., Doyle, F.J., III, Edwards, J.S., and Mahadevan, R., *Biotecnol. Bioeng.*, 2005, vol. 89, pp. 243–251.
27. Visser, D., Schmid, J.W., Mauch, K., Reuss, M., and Heijnen, J.J., *Metab. Eng.*, 2004, vol. 6, pp. 378–390.
28. Krömer, J.O., Wittmann, C., Schröoder, H., and Heinzle, E., *Metab. Eng.*, 2006, vol. 8, pp. 353–369.
29. Nikerel, I.E., Van Winden, W.A., Van Gulik, W.M., and Heijnen, J.J., *BMC Bioinformatics,* 2006, vol. 7, p. 540.
30. Van Dien, S.J., Iwatani, S., Usuda, Y., and Matsui, K.T., *J. Biosci. Bioeng.,* 2006, vol. 102, pp. 34–40.
31. Vital-Lopez, F.G., Armaou, A., Nikolaev, E.V., and Maranas, C.D., *Biotechnol. Prog.*, 2006, vol. 22, no. 6, pp. 1507–1517.
32. Young, J.D., Henne, K.L., Morgan, J.A., Konopka, A.E., and Ramkrishna, D., *Biotechnol. Bioeng.,* 2008, vol. 100, no. 3, pp. 5452–559.
33. Varma, A. and Palsson, B.O., *Appl. Environ. Mecrobiol.*, 1994, vol. 60, no. 10, pp. 3724–3731.
34. Varma, A. and Palsson, B.O., *Biotechnol. Bioeng.*, 1994, vol. 43, no. 4, pp. 275–285.
35. Varma, A. and Palsson, B.O., *Biotechnol. Bioeng.,* 1995, vol. 45, no. (1), pp. 69–79.
36. Pramanik, J. and Keasling, J.D., *Biotechnol. Bioeng.,* 1997, vol. 56, no. 4, pp. 398–421.
37. Ibarra, R.U., Edwards, J.S., and Palsson, B.O., *Nature*, 2002, vol. 420, pp. 186–189.
38. Reed, J.L., Vo, T.D., Schilling, C.H., and Palsson, B.O., *Genome Biol.*, 2003, vol. 4, no. 9, p. R54.
39. Nazipova, N.N., El'kin, Yu.E., Panyukov, V.V., and Drozdov-Tikhomirov, L.N., *Matem. Biol. Bioinform.*, 2007, vol. 2, pp. 98–119.
40. Llaneras, F. and Pico, J., *J. Biosci. Bioeng.*, 2008, vol. 105, pp. 1–11.
41. Drozdov-Tikhomirov, L.N., Scurida, G.I., and Serganova, V.V., *Biotechnologia* (Moskow), 1986, vol. 2, pp. 28–37.
42. Drozdov-Tikhomirov, L.N., Scurida, G.I., Davidov, A.V., Alexandrov, A.A., and Zvyagilskaya, R.A., *J. Bioinform. Comput. Biol.*, 2006, vol. 4, pp. 865–885.
43. Vallino, J.J. and Stephanopoulos, G., *Biotechnol. Bioeng.*, 1993, vol. 4, no. 6, pp. 633–646.
44. Papoutsakis, E.T., *Biotechnol. Bioeng.*, 1984, vol. 26, no. 2, pp. 174–187.
45. Desai, R.P., Nielsen, L.K., and Papoutsakis, E.T., *J. Biotechnol.,* 1999, vol. 71, pp. 191–205.
46. Desai, R.P., Harris, L.M., Welker, N.E., and Papoutsakis, E.T., *Metab. Eng.*, 1999, vol. 1, pp. 206–213.
47. Burgard, A.P., Pharkya, P., and Maranas, C.D., *Biotechnol. Bioeng.*, 2003, vol. 84, pp. 647–657.
48. Sanchez, A.M., Bennett, G.N., and San, K.Y., *Metab. Eng*, 2006, vol. 8, no. 3, pp. 209–226.
49. Pharkya, P., Burgard, A.P., and Maranas, C.D., *Biotechnol. Bioeng.,* 2003, vol. 84, pp. 887–899.
50. Fong, S.S., Burgard, A.P., Herring, C.D., Knight, E.M., Blattner, F.R., Maranas, C.D., and Palsson, B.O., *Biotechnol. Bioeng.*, 2005, vol. 91, pp. 643–648.
51. Hua, Q., Joyce, A.R., Fong, S.S., and Palsson, B.O., *Biotechnol. Bioeng.*, 2006, vol. 95, pp. 992–1002.
52. Edwards, J.S., Ibarra, R.U., and Palsson, B.O., *Nat. Biotechnol.*, 2001, vol. 19, pp. 125–130.
53. Watson, M.R., *Comput. Appl. Biosci.*, 1986, vol. 2, no. 1, pp. 23–27.
54. Ramakrishna, R., Edwards, J.S., McCulloch, A., and Palsson, B.O., *Am. J. Physiol. Regul. Integr. Physiol.*, 2001, vol. 280, no. 3, pp. R695–704.
55. Schiling, C.H., Covert, M.W., Famili, I., Church, G.M., Edwards, J.S., and Palsson, B.O., *J. Bacteriol.*, 2002, vol. 184, no. 16, pp. 4582–4593.
56. Resendis-Antonio, O., Reed, J.L., Encarnación, S., Collado-Vides, J., and Palsson, B.O., *PLoS Comput. Biol.,* 2007, vol. 3, no. 10, pp. 1887–1895.
57. Joyce, R.R. and Palsson, B.O., *Method Mol. Biol.*, 2008, vol. 416, pp. 433–457.58.Lee, J., Yun, H., Feist, A.M., Palsson, B.O., and Lee, S.Y., *Appl. Microbiol. Biotechnol.*, 2008, vol. 80, no. 5, pp. 849–862.
59. Pharkya, P., Burgard, A.P., and Maranas, C.D., *Genome Res.*, 2004, vol. 14, no. 11, pp. 2367–2376.
60. Kim, J.I., Varner, J.D., and Ramikrishna, D., *Biotechnol. Prog.*, 2008, vol. 24, no. 5, pp. 993–1006.
61. Chassagnole, C., Noisommit-Rizzi, N., Schmid, J.W., Mauch, K., and Reuss, M., *Biotechnol. Bioeng.*, 2002, vol. 79, pp. 53–73.
62. Hoefnagel, M.H., Starrenburg, M.J., Martens, D.E., Hugenholts, J., Kleerebezem, M., Van Swam, I.I.,

Bongers, R., Westerhoff, H.V., and Shoep, J.L., *Microbiology,* 2002, vol. 148, pp. 1003–1013.

63. Bruggeman, F.J., Boogerd, F.C., and Westerhoff, H.V., *FEBS J.*, 2005, vol. 272, pp. 1965–1985.
64. Heijnen, J.J., *Biotechnol. Bioeng.*, 2005, vol. 91, pp. 534–545.
65. Heinrich, R., Rapoport, S.M., and Rapoport, T.A., *Prog. Biophys. Mol. Biol.,* 1977, vol. 32, pp. 1–2.
66. Hatzimanikatis, V., Floudas, C.A., and Bailey, J.E., *AIChE J.*, 1996, vol. 42, pp. 1277–1292.
67. Nielsen, J., *Biochem. J.,* 1997, vol. 321, pp. 133–138.
68. Visser, D. and Heijnen, J.J., *Metab. Eng.*, 2003, vol. 5, no. 3, pp. 164–176.
69. Wu, L., Wang, W., van Winden, W.A., van Gulik, W.M., and Heijnen, J.J., *Eur. J. Biochem.*, 2004, vol. 271, non. 16, pp. 3348–3359.
70. Nikerel, I.E., Van Winde, W.A., Verheijen, P.J., and Heijnen, J.J., *Metab. Eng.*, 2009, vol. 11, pp. 20–30.
71. Voit, E.O. and Savageau, M.A., *Biochemistry*, 1987, vol. 26, no. 21, pp. 6869–6880.
72. Shiraishi, F. and Savageau, M.A., *J. Biol. Chem.*, 1992, vol. 267, pp. 22912–22918.
73. Hernandez-Bermejo, B., Fairen, V., and Sorribas, A., *Math. Biosci.,* 1999, vol. 16, pp. 83–94.
74. Hernandez-Bermejo, X.B., Fairen, V., and Sorribas, A., *Math. Biosci.*, 2000, vol. 167, pp. 87–107.
75. Likhoshvai, V.A., Ignat'eva, E.V., and Podkolodnaya, O.A., *Izv. Akad. Nauk, Ser. Biol.*, 2001, vol. 35, pp. 1072–1079.
76. Likhoshvai, V.A., Ratushnyi, A.V., Bazhan, S.I., Oshchepkova, E.A., Fadeev, S.I., Khlebodarova, T.M., and Kolchanov, N.A., *Metody modelirovaniya dinamiki molekulyarno-geneticheskikh sistem. Sistemnaya komp'yuternaya biologiya* (Dynamics Simulation Methods for Molecular–Genetic Systems. Systemic Computer Biology), Kolchanov, N.A., Goncharov, S.S., Likhoshvay, V.A., and Ivanisenkov, V.A., Eds., Novosibirsk: Izd. SO RAN, 2008, pp. 333–393.
77. Likhoshvai, V. and Ratushny, A., *J. Bioinform. Comput. Biol.*, 2007, vol. 5, pp. 521–531.
78. Likhoshvai, V. and Ratushny, A., *Proc. of the Fifth International Conference on Bioinformatics of Genome Regulation and Structure, BGRSX2006,* Kolchanov, N. et al., Eds., Novosibirsk: IC&G Press, 2006, vol. 2, pp. 13–18.
79. Ratushny, A.V., Nedosekina, E.A., Lashin, S.A., Turnaev, I.I., Vladimirov, N.V., Podkolodnyi, N.L., and Likhoshvai, V.A., *Baza matematicheskikh modelei molekulyarno-geneticheskikh protsessov (ModelER)* (Base of Mathematical Models of Molecular-Genetic Processes (ModelER)), RF Inventor's Certificate no. 2006620196, 2006.
80. Khlebodarova, T.M., Lashin, S.A., and Apasieva, N.V., *Proc. of the Fifth International Conference on Bioinformatics of Genome Regulation and Structure, BGRSX2006,* Kolchanov, N. et al., Eds., Novosibirsk: IC&G Press, 2006, vol. 2, pp. 55–59.
81. Ratushny, A., Usuda, Y., Matsui, K., and Podkolodnaya, O.A., *Proc. of the Fifth International Conference on Bioinformatics of Genome Regulation and Structure, BGRSX2006,* Kolchanov, N. et al., Eds., Novosibirsk: IC&G Press, 2006, vol. 2, pp. 25–29.
82. Oshchepkova-Nedosekina, E.A. and Likhoshvai, V.A., *Theor. Biol. Med. Model.*, 2007, vol. 4, p. 11.
83. Cornish-Bowden, A., *Biochem. J.*, 1977, vol. 165, pp. 55–59.
84. Akowski, J.P. and Bauerle, R., *Biochemistry*, 1997, vol. 36, pp. 15817–15822.
85. Hochstadt-Ozer, J. and Stadtman, E.R., *J. Biol. Chem.*, 1971, vol. 246, pp. 5294–5303.
86. Tarmy, E.M. and Kaplan, N.O., *J. Biol. Chem.*, 1968, vol. 243, pp. 2587–2596.
87. Jiang, G.R., Nikolova, S., and Clark, D.P., *Microbiology*, 2001, vol. 147, pp. 2437–2446.
88. Wilson, H.R., Archer, C.D., Liu, J.K., Turnbough, C.L., Jr., *J. Bacteriol.*, 1992, vol. 174, pp. 514–524.
89. Hommais, F., Krin, E., Coppee, J.Y., Lacroix, C., Yeramian, E., Danchin, A., and Bertin, P., *Microbiology*, 2004, vol. 150, pp. 61–72.
90. Spiro, S. and Guest, J.R., *Trends Biochem. Sci.*, 1991, vol. 16, no. 8, pp. 310–314.
91. Cotter, P.A. and Gunsalus, R.P., *FEMS Microbiol. Letts.*, 1992, vol. 70, pp. 31–36.
92. Lynch, A.S. and Lin, E.C., *J. Bacteriol.*, 1996, vol. 178, no. 21, pp. 6238–6249.
93. Salmon, K.A., Hung, S.P., Steffen, N.R., Krupp, R., Baldi, P., Hatfield, G.W., and Gunsalus, R.P., *J. Biol. Chem.,* 2005, vol. 280, no. 15, pp. 15084–15996.
94. Tseng, C.P., Albrecht, J., and Gunsalus, R.P., *J. Bacteriol.,* 1996, vol. 178, pp. 1094–1098.
95. Compan, I. and Touati, D., *Mol. Microbiol.*, 1994, vol. 11, no. 5, pp. 955–964.
96. Robin, J.P., Penverne, B., and Herve, G., *Eur. J. Biochem.*, 1989, vol. 183, pp. 519–528.
97. De Staercke, C., Van Vliet, F., Xi, X.G., Rani, C.S., Ladjimi, M., Jacobs, A., Triniolles, F., Herve, G., and Cunin, R., *J. Mol. Biol.,* 1995, vol. 246, pp. 132–143.
98. Wild, J.R., Loughrey-Chen, S.J., and Corder, T.S., *Proc. Natl. Acad. Sci. USA*, 1989, vol. 86, pp. 46–50.
99. Daniel, R., Kokel, B., Caminade, E., Martel, A., and Le Goffic, F., *Anal. Biochem.,* 1996, vol. 239, pp. 130–135.
100. Bjornberg, O., Gruner, A.C., Roepstorff, P., and Jensen, K.F., *Biochemistry*, 1999, vol. 39, pp. 2899–2908.
101. Shimosaka, M., Fukuda, Y., Murata, K., and Kimura, A., *J. Bacteriol.*, 1984, vol. 160, pp. 1101–1104.
102. Donovan, W.P. and Kushner, S.R., *J. Bacteriol.*, 1983, vol. 156, pp. 620–624.
103. Bucurenci, N., Serina, L., Zaharia, C., Landais, S., Danchin, A., and Barzu, O., *J. Bacteriol.*, 1998, vol. 180, pp. 473–477.

104. Ginther, C.L. and Ingraham, J.L., *J. Biol. Chem.*, 1974, vol. 249, pp. 3406–3411.

105. MacDonnell, J.E., Lunn, F.A., and Bearne, S.L., *Biochim. Biophys. Acta*, 2004, vol. 1699, pp. 213–220.

106. Villadsen, I.S. and Michelsen, O., *J. Bacteriol.*, 1977, vol. 301, pp. 136–143.

107. Teusink, B., Larsson, C., Diderich, J., Richard, P., van Dam, K., Gustafsson, L., and Westerhoff, H.V., *J. Biol. Chem.*, 1996, vol. 27, pp. 24442–24448.

108. Higgins, J., *Proc. Natl. Acad. Sci. USA*, 1964, vol. 51, pp. 989–994.

109. Carre, I.A. and Edmunds, L.N., Jr., *J. Cell. Sci.*, 1993, vol. 104, pp. 1163–1173.

110. Likhoshvai, V.A., Kazantsev, F.V., Akberdin, I.R., Bezmaternykh, K.D., Lashin, S.A., Podkolodnaya, N.N., and Ratushny, A.V., Computer System for Constructing, Computation, and Analysis of Molecular-Genetic System Models (MGSmodeller), RF Inventor's Certificate no. 2008612820, 2008.

111. Likhoshvai, V.A., Khlebodarova, T.M., and Kolchanov, N.A., *Ekologicheskaya, biotekhnologicheskaya, meditsinskaya i teoreticheskaya mikrobiologiya* (Ecological, Biogtechnological, Medicinal, and Theoretical Microbiology), Vlasov, V.V., Degermendzhi, A.G., Kolchanov, N.A., Parmon, V.N., and Repin, V.E., Eds., Novosibirsk: Izd. SO RAN, 2009, pp. 277–290 (in press).